Electron beam probing of silica surface layers on alumina

Nadège Cornet, Dominique Goeuriot, Matthieu Touzin, Christelle Guerret-Piecourt, Denyse Juvé, Daniel Tréheux, Hans-Joachim Fitting

Electron beam probing of silica surface layers on alumina

N. Cornet [a], D. Goeuriot [a], M. Touzin [b], C. Guerret-Piécourt [c], D. Juvé [c], D. Tréheux [c], H.-J. Fitting [d,*]

[a] *Ecole Nationale Supérieure des Mines, 158 cours Fauriel, F-42023 Saint-Etienne, France*
[b] *Université des Sciences et Technologies de Lille, F-59655 Villeneuve d'Ascq, France*
[c] *Ecole Centrale de Lyon, 36 Avenue Guy de Collongue, F-69134 Ecully, France*
[d] *Institue of Physics, University of Rostock, Universitaetsplatz 3, D-18051 Rostock, Germany*

The electron beam induced self-consistent charge injection and transport in a layered insulator SiO_2–Al_2O_3 is described by means of an electron–hole flight–drift model FDM and an iterative computer sim-ulation. Thermal and field-enhanced detrapping are included by the Poole–Frenkel effect. The surface layer with a modified electric surface conductivity is included which describes the surface leakage cur-rents. Furthermore, it will lead to particular charge incorporation at the interface between the surface layer and the bulk substrate. As a main result the time-dependent spatial distributions of currents $j(x,t)$, charges $\rho(x,t)$, field $F(x,t)$, and potential $V(x,t)$ are obtained. The spatial charge distribution with depth shows a quadro-polar plus–minus–plus–minus structure in nanometer dimension.

1. Introduction

The scaling down of electronic devices results in a constant decrease of the involved dielectric thickness leading to various problems of physical limits such as high leakage currents or breakdown phenomena. The use of modified surface layers or thin film depositions are classical solution to reach the limited thickness or mass reduction while avoiding the problems mentioned above [1,2]. For a better understanding of these phenomena of charge transport in insulators a physical model and a computer simulation will be set up in the present paper. Indeed, thanks to a flight–drift model (FDM) of injected electrons and holes in insulators and an iterative computer simulation an understanding of the self-consistent charge transport in bulk insulating samples is possible [3–5].

The aim of the present work is to show the influence of a silica (SiO_2) surface layer on the electron and hole injection, drift and trapping, on the secondary electron emission, and on the spatial charge distribution in alumina (Al_2O_3) bulk samples.

2. Theoretical background

The problem of electron beam charge injection in a heterogeneous layered target is demonstrated in Fig. 1. Incident electrons (so-called primary electrons PE) with initial energy E_0 and current density j_0 penetrate the insulator target up to the maximum range $R(E_0)$:

$$R_{SiO_2} = 33.7(E_0/\mathrm{keV})^{1.55}, \tag{1a}$$

$$R_{Al_2O_3} = 28.7(E_0/\mathrm{keV})^{1.55}, \tag{1b}$$

where R is given in nm, and the electron beam energy E_0 should be inserted in keV [6]. The flight–drift model (FDM) with the scattering and straggling of primary electrons (PE), their excitation of secondary electrons (SE) and holes (SH), their ballistic flight as ballistic

* Corresponding author. Tel.: +49 381 498 6760; fax: +49 381 498 6802.
E-mail address: hans-joachim.fitting@uni-rostock.de (H.-J. Fitting).

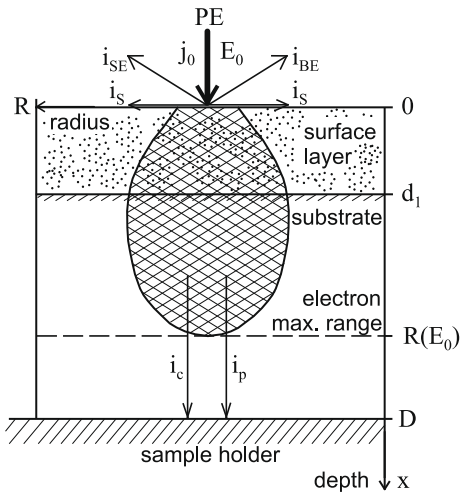

Fig. 1. Primary electron (PE) injection into a layered target with a surface layer d_1 and an overall sample thickness D; the interaction volume (hatched) is extended to the maximum electron range $R(E_0)$ with following currents: i_{BE}: backscattered electron, i_{SE}: secondary electrons, i_S: surface current, i_c: possible real conduction current, i_p : polarization displacement current.

electrons (BE) and holes (BH), respectively, their attenuation and drift as drifting electrons (DE) and holes (DH) in self-consistent fields, followed by recombination and/or trapping and detrapping in localized states (traps) is presented schematically in Fig. 2. All these processes are included in the following Eq. (5) for drifting electrons (DE) in reverse (R) direction towards the surface and transmission (T) directions into the sample volume (bulk):

$$
\begin{aligned}
j^{\mathrm{DER}}_{\mathrm{DET}}(x) = \Big\{ & j^{\mathrm{DER}}_{\mathrm{DET}}(x \pm \Delta x) + [j_{\mathrm{BER}}(x)[1 - W_{\mathrm{EFR}}(x)] + j_{\mathrm{BET}}(x)[1 - W_{\mathrm{EFT}}(x)] \\
& + \text{convection generation by ballistic attenuation} \\
& + \varrho_{\mathrm{E1}}(x) W_{\mathrm{E1PF}} + \varrho_{\mathrm{E2}}(x) W_{\mathrm{E2PF}}] \times F_{\mathrm{E}}(x) \Big\} \\
& \times \text{detrapping by Poole—Frenkel effect} \\
& \times \underbrace{\exp\left[-\left(N_1 - \frac{\varrho_{\mathrm{E1}}}{e_0}\right) S_{\mathrm{E1}} \Delta x\right]}_{W_{\mathrm{E1}}} \cdot \underbrace{\exp\left[-\left(N_2 - \frac{\varrho_{\mathrm{E2}}}{e_0}\right) S_{\mathrm{E2}} \Delta x\right]}_{W_{\mathrm{E2}}} \\
& \times \text{trapping in shallow}^{(1)} \text{and deep}^{(2)} \text{states} \\
& \times \underbrace{\exp\left[-\frac{\varrho_{H1}}{e_0} S_{\mathrm{EH1}} \Delta x\right]}_{W_{\mathrm{EH1}}} \cdot \underbrace{\exp\left[-\frac{\varrho_{H2}}{e_0} S_{\mathrm{EH2}} \Delta x\right]}_{W_{\mathrm{EH2}}} \\
& \times \text{recombination with holes.}
\end{aligned}
\tag{2}
$$

Here the first convection term describes incoming and outgoing drifting electrons in the depth element Δx; the second generation term presents the sources of drifting electrons by attenuated (exhausted) ballistic electrons; the third (detrapping) term is given by the Poole–Frenkel release of electrons from traps, presenting also a source of drifting electrons. The field factor F_{E} describes the anisotropy of all generated drifting electrons (DE) in the electric field F. Finally, as electron drains we see the trapping and recombination terms with trap concentrations N and actual charges ϱ as well as the respective cross sections S, all as presented in Fig. 2. Of course, the current density equation $j^{\mathrm{DHR}}_{\mathrm{DHT}}$ for drifting holes (DH) looks adequate with the respective trapping parameters of holes, as already described in [4].

Further on, the Poole–Frenkel release [7,8] of charges from traps is given by:

$$
W^{\mathrm{HPF}}_{\mathrm{EPF}} = f^{\mathrm{H}}_{\mathrm{E}} \exp\left[-\frac{E^{\mathrm{H}}_{\mathrm{E}} - \Delta E_{\mathrm{PF}}}{kT}\right], \tag{3}
$$

for electrons (E) and holes (H), respectively. This enhanced charge release from traps is due to a trap barrier lowering ΔE_{PF} by an electric field F [8]:

$$
\Delta E_{\mathrm{PF}} = 2 \frac{e^{3/2}}{(4\pi\varepsilon_0\varepsilon_r)^{1/2}} F^{1/2} = \beta_{\mathrm{PF}} F^{1/2}. \tag{4}
$$

The resulting charges will be counted from the balance of trapping and detrapping: $\varrho(x,t) = -\varrho_{\mathrm{E1}} - \varrho_{\mathrm{E2}} + \varrho_{\mathrm{H1}} + \varrho_{\mathrm{H2}}$. On the other hand, we may account the charges and the fields from current fluctuations (divergences) too:

$$
-\frac{\partial}{\partial x} j(x,t) = \frac{\partial \varrho(x,t)}{\partial t} = \varepsilon_0 \varepsilon_r \frac{\partial}{\partial t} \frac{\partial}{\partial x} F(x,t), \tag{5}
$$

as it has been already described more detailed in Ref. [4].

3. Results and discussion

The general computation scheme for the self-consistent charging has been presented already in [4]. The simulations for layered targets were performed for 3 mm bulk Al_2O_3 samples covered by a 1 μm SiO_2 surface layer, see Fig. 1. First of all we want to check the total SE emission rate $\sigma = \eta + \delta$ of backscattered (η) and true secondary electrons (δ) released from the target material. For bulk insulating samples and no electrical conduction to the support this rate σ should approach the value 'one' in stationary saturation state, $\sigma(t) \to 1$, i.e., currents of injected primary electrons (PE) j_0

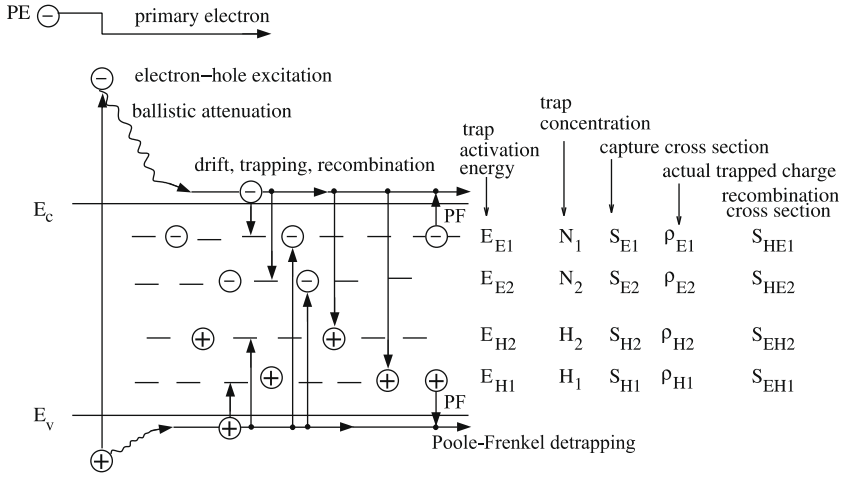

Fig. 2. Scheme of the flight–drift model (FDM) including the excitation of ballistic electrons and holes, their flight and attenuation, followed by drift or diffusion, trapping or recombination.

and emitted backscattered and secondary electrons j_{SE} compensate each other and the final stationary state with $j(x,t) = 0$ is reached.

In Fig. 3 (top) we see that this steady stationary state is reached after (20–50) ms electron beam injection with $E_0 = 20$ keV and $j_0 = 10\ \mu A/cm^2$ at room temperature $T = 300$ K. It means that for this temperature the supposed surface traps with thermal activation energy $E_S \cong 0.2$ eV are not yet activated and the surface charges remain still localized. Increasing the sample temperature T to 500 and 1000 K we observe a lower saturation value of $\sigma(t) < 1$ with an indication of a surface leakage current $j_S > 0$ due to the increasing mobility of the surface charges.

The negative surface potential $V_0(t)$ is presented in the lower part of Fig. 3. There the maximum negative value $V_0 \approx -15$ kV is reached already after $t = 17$ ms injection but then a slight decrease due to surface charge release and surface leakage current $j_S(t)$ is observed leading finally also to a steady saturation state with a surface potential of about $V_0(t > 70\ \text{ms}) \approx 12.5$ kV for a high temperature of $T = 1000$ K. Obviously, this behavior of the both experimentally accessible quantities, the SE rate σ and the surface potential V_0, offers the possibility to compare and characterize insulators with respect to their electrical features.

The peculiarity of the layered sample with a surface layer of thickness d_1 on a bulk substrate is the interface between both in the depth d_1 as shown in Fig. 1. Within the more dense material Al_2O_3 the spatial concentration of electrons and holes is higher than in SiO_2 leading to a jump of currents across the interface at

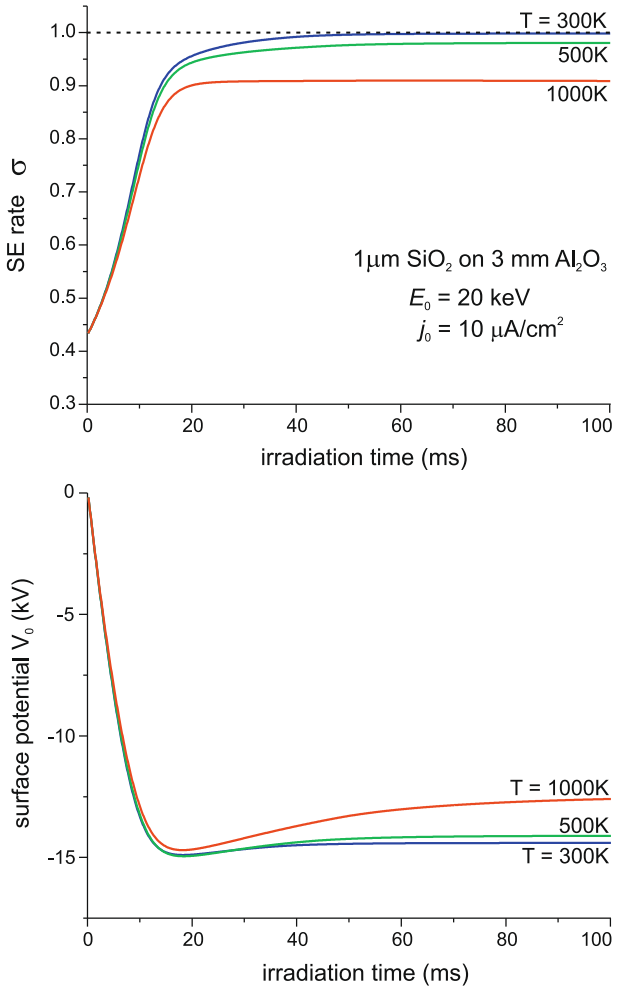

Fig. 3. Total SE rate $\sigma(t)$ and surface potential $V_0(t)$ as a function of irradiation time t and sample temperature T; sample: 1 μm SiO_2 layer on 3 mm Al_2O_3; electron beam: $E_0 = 20$ keV; $j_0 = 10\ \mu A/cm^2$.

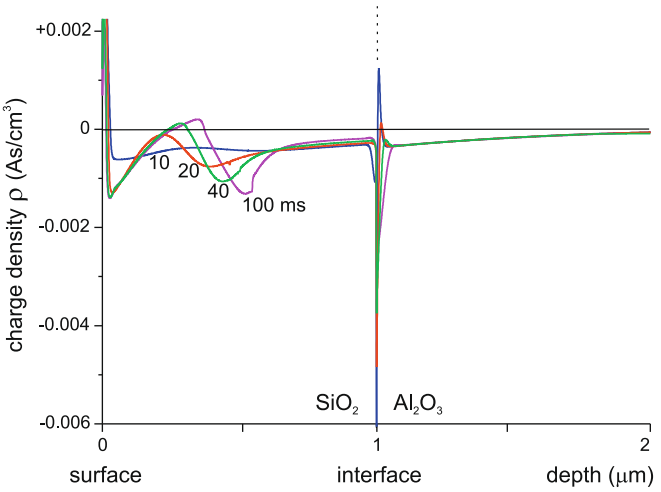

Fig. 4. Charge distribution (profile) within a SiO_2–Al_2O_3 sample injected by an electron beam of $E_0 = 20$ keV.

d_1. Consequently, a bipolar minus–plus spatial charge distribution is built up at the interface d_1, as to be seen in Fig. 4. With ongoing electron beam injection the internal total current density $j(x,t)$ will be flattened and finally approaching the value zero over all depths x: $j(x,\infty) \to 0$. This corresponds to the steady stationary state $\sigma = 1$. The respective charge distributions in Fig. 4 show a typical plus–minus–plus–minus quadro-polarity as already described in Refs. [4,5]. The reason for that is the electric field distribution $F(x)$ in plus–minus bipolarity separating electrons and holes in one and the other direction. More details can be found in Ref. [5].

4. Conclusions

Electron beam charge injection is associated by self-consistent charge transport in insulating and dielectric samples and described by an electron–hole flight–drift model (FDM) implemented by an iterative computer simulation. Ballistic electrons and holes are followed down to their attenuation and drift, their possible recombination or trapping in shallow and deep traps. Furthermore a detrapping by the temperature- and field-dependent Poole–Frenkel effect becomes possible allowing even a charge hopping transport. In this context a special SiO_2 surface layer has been installed to investigate the effect of surface leakage currents.

As a main result the spatial distributions of currents $j(x,t)$, charges $\rho(x,t)$, electric field $F(x,t)$, and potential $V(x,t)$ are obtained in a self-consistent procedure as well as the time dependent secondary electron emission rate $\sigma(t)$ and surface potential $V_0(t)$ both experimentally accessible. For bulk full insulating samples the above quoted time-dependent distributions approach the final stationary state under the condition $j(x,t) = \text{const} = 0$ and $\sigma = 1$. In case of remarkable surface leakage current i_S the steady stationary final state is obtained with $\sigma < 1$. Generally we obtain a plus–minus–plus–minus spatial charge distribution with prevailing minus parts within the bulk insulator produced by a bipolar field: a positive field near the surface and a negative one in the remaining bulk. Thus, due to drift processes of electrons and holes the opposite charge separations lead to the quadro-polarized charge structure across the sample depth.

First experimental results of $\sigma(t)$, $V_0(t)$ and instationary sample i_{sc} and surface i_s current measurements are still in sufficient agreement with this self-consistent charge transport simulation, see more in [3,5]. Such investigations offer the opportunity to characterize insulating materials with respect to their quality, their electrical behavior, and radiation resistance.

References

[1] R.G. Vitchev, J.J. Pireaux, T. Conard, H. Bender, J. Wolstenholme, C. Defranoux, Appl. Surf. Sci. 235 (2004) 21.
[2] D.C. Ferguson, G.B. Hillard, NASA Reports, TP-2003-212287, 2003.
[3] X. Meyza, D. Goeuriot, C. Guerret-Piécourt, D. Tréheux, H.-J. Fitting, J. Appl. Phys. 94 (2003) 5384.
[4] M. Touzin, D. Goeuriot, C. Guerret-Piécourt, D. Juvé, D. Tréheux, H.-J. Fitting, J. Appl. Phys. 99 (2006) 114110.
[5] N. Cornet, D. Goeuriot, C. Guerret-Piécourt, D. Juvé, D. Tréheux, M. Touzin, H.-J. Fitting, J. Appl. Phys. 103 (2008) 064110-1.
[6] H.-J. Fitting, N. Cornet, Roushdey Salh, C. Guerret-Piécourt, D. Goeuriot, A. von Czarnowski, J. Electron Spectrosc. Rel. Phenom. 159 (2006) 46.
[7] J. Frenkel, Phys. Rev. 54 (1938) 647.
[8] J.J. O'Dwyer, The Theory of Electrical Conduction and Breakdown in Solid Dielectrics, Clarendon, Oxford, 1973.